JOC The Journal of Organic Chemistry

Article

pubs.acs.org/joc

Synthesis, Rotational Dynamics, and Photophysical Characterization of a Crystalline Linearly Conjugated Phenyleneethynylene Molecular Dirotor

Melissa Hughs, Miguel Jimenez, Saeed Khan, and Miguel A. Garcia-Garibay*

Department of Chemistry and Biochemistry, University of California, Los Angeles, California 90095-1569, United States

Supporting Information

ABSTRACT: We report the synthesis, crystal structure, solid-state dynamics, and photophysical properties of 6,13-bis((4-(3-(3-methoxyphenyl)-3,3-diphenylprop-1-yn-1-yl)phenyl)-ethynyl)-5,7,12,14-tetrahydro-5,14:7,12-bis([1,2]benzeno)pentacene (**1**), a molecular dirotor with a 1,4-bis((4-ethynylphenyl)ethynyl)benzene (BEPEB) chromophore. The incorporation of a pentiptycene into the molecular dirotor provides a central stator and a fixed phenylene ring relative to which the two flanking ethynylphenylene rotators can explore various torsion angles; this allows the BEPEB fluorophore dynamics to persist in the solid state. X-ray diffraction studies have shown that molecular dirotor **1** is packed so that all the BEPEB fluorophores adopt a parallel alignment, this is ideal for the development of functional materials. Variable temperature, quadrupolar echo ^{2}H NMR studies have shown that phenylene rotator flipping has an activation energy of 9.0 kcal/mol and a room temperature flipping frequency of ~2.6 MHz. Lastly, with measurements in solution, glasses, and crystals, we obtained evidence that the fluorescence excitation and emission spectra of the phenyleneethynylene chromophores is dependent on the extent of conjugation between the phenylene rings, as determined by their relative dihedral angles. This work provides a promising starting point for the development of molecular dirotors with polar groups whose amphidynamic nature will allow for the rapid shifting of solid-state absorption, fluorescence, and birefringence, in response to external electric fields.

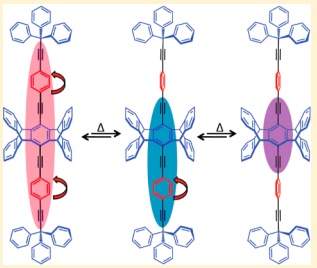

INTRODUCTION

Recent advances in the fields of functional materials and artificial molecular machines[1] have led to the development of crystalline molecular machinery,[2] which is intended to take advantage of internal molecular motion, and/or chemical reactivity, to influence mechanical properties,[3] electric,[4] magnetic,[5] and/or optical functions[6] in a highly controlled and anisotropic manner. Over the past few years, our group has emulated the structures of macroscopic gyroscopes, as they are useful models for the design of molecules capable of forming amphidynamic crystals with static elements and rapidly moving parts.[2] Like their macroscopic namesakes, molecular gyroscopes consist of a central rotator linked by an axle to two shielding stator groups that are responsible for self-assembly of an ordered crystal lattice. The rotational dynamics of these molecules in the solid-state depends on the nature of the stator, the rotator size and symmetry, and the details of the crystal packing.[7] Using frequency-dependent dielectric spectroscopy as a function of temperature, we showed that molecular gyroscopes with rotators bearing a permanent dipole moment can be interfaced with external AC fields.[4c] In this study we report a structural motif whose rotational dynamics are expected to allow for the incorporation of optical functions into the bulk crystalline material. Specifically we have modified the common 1,4-diethynylbenzene rotator motif for one that contains two rotators linearly conjugated with a phenyl ring at the center, which is part of a pentiptycene stator. The desired dirotor has a 1,4-bis((4-ethynylphenyl)ethynyl)benzene (BEPEB) chromophore (Figure 1). Based on the well-known changes in the photophysical properties of these structures as a function of aromatic group planarization and twisting,[8,9] we expect that changes in conjugation brought about by changes in the orientation of the moving phenylene rotators will result in solid-state spectral shifts that will be useful for the generation of a new class of optical materials. As shown in the top portion of Figure 1, the chromophore may vary from a fully coplanar 1,4-bis(4-ethynylphenyl)ethynyl)benzene (BEPEB, shown in blue) to structures that have one or two rings out of conjugation, which result in chromophores analogous to 1,2-bis(4-ethynylphenyl)ethyne (BEPE, shown in purple) and 1,4-diethynylbenzene (DEB, shown in violet).

Linearly conjugated phenyleneethynylenes are remarkable chromophores. Their three aromatic rings experience nearly barrierless rotation in the ground state but have large energy variations as a function of their dihedral angle in the excited state.[8,9,15] The difference between the ground- and excited-state rotational potentials is the result of changes in bond order, as the single and triple bonds linking the aromatic groups in the ground state acquire the character of an extended cummulene upon electronic excitation. It has been shown that coplanar conformations of 1,4-bis(arylethynyl)benzene display red shifts of ca. 20−30 nm in absorption and emission as compared to "twisted" conformers where the plane of the central ring is

Received: March 2, 2013
Published: May 7, 2013

dx.doi.org/10.1021/jo4004053 | J. Org. Chem. 2013, 78, 5293−5302

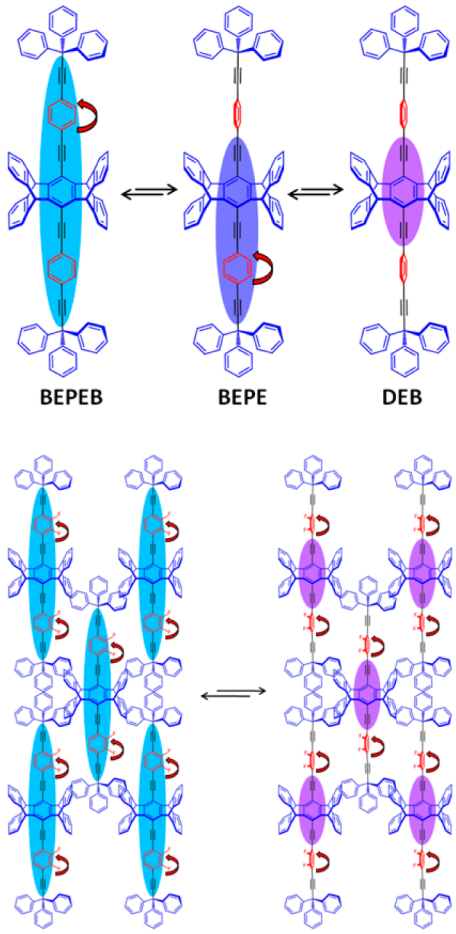

Figure 1. Top: Rotation of the phenylene rotators in a phenyleneethynylene molecular dirotor reveals chromophores with varying degrees of π-conjugation; the chromophore may vary from a fully coplanar 1,4-bis((4-ethynylphenyl)ethynyl)benzene (BEPEB, shown in blue) analogue to a partially conjugated 1,2-bis(4-ethynylphenyl)-ethyne (BEPE, shown in purple) analogue or an unconjugated 1,4-diethynyl benzene (DEB, shown in violet) analogue. Bottom: An idealized crystal where polar (2,3-difluorophenylene) rotators are able to reorient as a function of an external electric field to change the optical properties of the material.

twisted with respect to the planes of the rings on the sides.[8] Elegant studies as a function of temperature by Yang and co-workers with a series of pentiptycene-derived oligo(*p*-phenyleneethynylene)s with significant intrachain interactions showed remarkable shifts as the emission changes from an excited-state population of mainly twisted conformers at low temperatures to one that consists of mainly coplanar structures as the temperature increases.[9] By incorporating two smaller phenylene rotators with one bulky pentypticene and two shielding trityl groups within the structure of a BEPEB fluorophore, we expect two phenylene rings will preserve some freedom of rotation in the solid state. Figure 1 (top) shows the suggested pentiptycene structure with two central 2,3-difluorophenylene rotators flanked by two triphenylmethyl stators. The hypothesized changes in excitation energy as a function of planarization for the idealized chromophore are qualitatively expected to resemble the BEPEB, BEPE, and DEB chromophores highlighted in blue, purple, and violet, respectively.

Shown in the bottom part of Figure 1 is an idealized crystal of the desired molecular dirotors. The application of a strong electric field is expected to influence the orientation and torsion angle of the dipolar 2,3-difluorophenylenes in and out of the plane of the pentiptycene central ring. While changes in the direction along the preferred orientation have the potential of breaking a centrosymmetric arrangement in the structure, changes in the orientation of the rotators can affect the conjugation of the chromophore, resulting in both nonlinear optical effects and changes in color (absorption spectra), as well as changes in dichroism and birefringence. While this behavior is reminiscent of the function of a liquid crystal,[10] suitable stator and rotator combinations in the solid state should lead to essentially barrierless rotation and optical switching at time scales that are only limited by the moment of inertia of the rotator (ca. 10^{-12} s), which is 6 to 9 orders of magnitude faster than the time scale required for domain reorientation in a liquid crystal.[10] While we have yet to achieve a true inertial rotator, we have previously measured rotation barriers as low as 1.48 kcal/mol, with a room temperature rotation frequency in the range of ~1−4.3 GHz.[11]

In this Article we report the synthesis, solid-state dynamics, and photophysical properties of the BEPEB molecular dirotor **1** shown in Scheme 1. Compound **1** was synthesized with a *m*-

Scheme 1

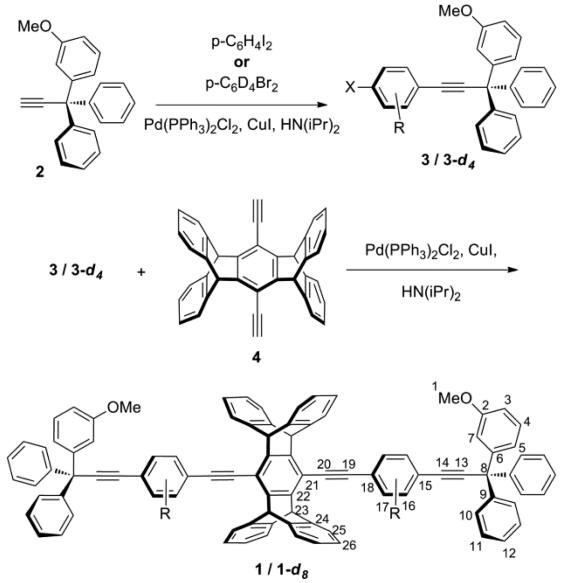

methoxy group in each of the two trityl stators to increase its solubility. Samples of the isotopologue, **1**-d_8, with deuterated phenylene rotators were obtained to allow for the determination of the phenylene rotational barrier in the solid state using quadrupolar echo ^{2}H NMR line-shape analysis experiments.[12,13] We confirmed that the relatively large aspect ratio of the desired molecular structure yields crystals with all the chromophores aligned in the same direction, which is ideal for the preparation of functional materials addressable by external electric fields. In addition, we showed that phenylene rotation is facile at ambient temperature (298 K) with a phenylene 180° jump average frequency of 2.6 MHz. Lastly, we showed that the BEPEB chromophore displays a reasonably strong emission that is homogeneous in a dilute toluene solution at room temperature but becomes highly heterogeneous in a rigid glass

dx.doi.org/10.1021/jo4004053 | J. Org. Chem. 2013, 78, 5293−5302

Scheme 2

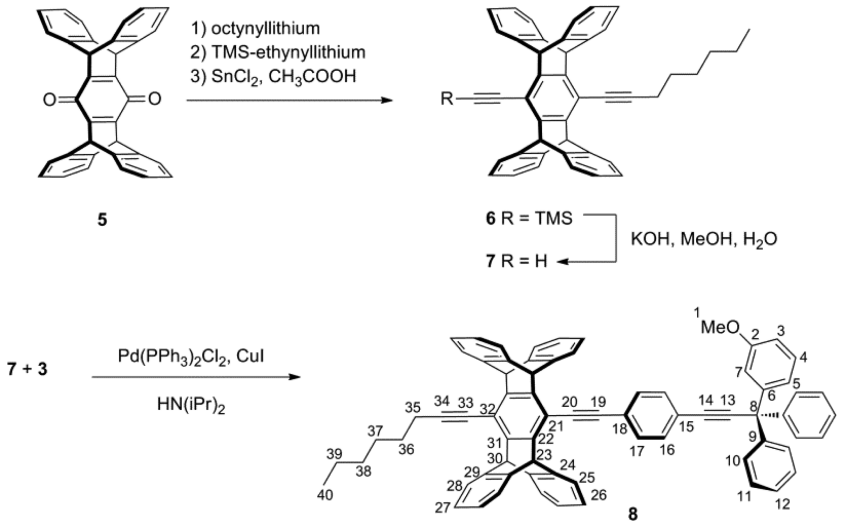

at 77 K. Clear evidence for the range of chromophores suggested in Figure 1 was obtained by analyzing the emission spectra as a function of excitation wavelength in the rigid glass, which revealed spectra that are nearly identical to those obtained from simple 1,4-diethynylbenzene (DEB), 1,2-bis(4-ethynylphenyl)ethyne (BEPE), and 1,4-bis((4-ethynylphenyl)-ethynyl)benzene (BEPEB). We confirmed that pentiptycene dirotors provide a promising platform for the development of solid-state functional materials with shifting absorption and emission properties with the application of external electric fields.

RESULTS AND DISCUSSION

Synthesis and Spectroscopic Characterization. The synthesis of the BEPEB molecular dirotor **1** was accomplished in a convergent manner, relying on previously developed procedures.[14] Samples of 3-(*m*-methoxyphenyl)-3,3-diphenyl-prop-1-yne **2** were obtained as described recently by our group. The central 6,13-diethynyl-5,7,12,14-tetrahydro-5,14:7,12-bis-([1,2]benzeno)pentacene **4** was prepared as reported by Swager and Yang.[15] As illustrated in Scheme 1, samples of 1-(3-(*m*-methoxyphenyl)-3,3-diphenylprop-1-ynyl)-4-iodobenzene **3** and its 4-bromo-phenylene deuterated analogue **3**d_4 were prepared via a Pd(0)-catalyzed Sonogashira coupling of **2** with either 1,4-diiodobenzene or 1,4-dibromobenzene-d_4 in refluxing 2:1 THF:diisopropylamine. Another Pd(0)-catalyzed coupling reaction using 3 equiv of **3** or **3**-d_4 per equivalent of **4** yielded BEPEB dirotors **1** and **1**-d_8, respectively. To have a model chromophore for photophysical studies, 6-((4-(3-(3-methoxyphenyl)-3,3-diphenylprop-1-yn-1-yl)phenyl)ethynyl)-13-(oct-1-yn-1-yl)-5,7,12,14-tetrahydro-5,14:7,12-bis([1,2]-benzeno)pentacene **8** was prepared as shown in Scheme 2. Pentiptycene quinone **5** was reacted subsequently with 1-octynyllithium and lithium TMS-acetylide to yield an asymmetrical diol which was immediately rearomatized with tin(II)chloride and deprotected with potassium hydroxide. The resulting asymmetrical diyne **7** was coupled to 1-(3-(*m*-methoxyphenyl)-3,3-diphenylprop-1-ynyl)-4-iodobenzene **3** via a Pd(0)-catalyzed Sonogashira reaction.

Both the ^{1}H and the ^{13}C NMR spectra of compounds **1**, **1**-d_8, **3**, **3**-d_4, and **8** possess all the signals expected from a mono *m*-methoxyphenyl trityl group with chemical shifts that are well conserved across the five structures. In the ^{1}H NMR spectrum of **1**, a singlet assigned to the methoxy groups is observed at 3.79 ppm, two doublet of doublet of doublets at ca. 6.70 and 6.90 ppm are assigned to the protons that are ortho and para to the methoxy group (H3 and H5 in Scheme 1), respectively. A doublet of doublets corresponding to H7 appears at 6.93 ppm and an apparent triplet at 7.23 ppm that is assigned to H4 complete the description of the *m*-methoxyphenyl group. The signals corresponding to the protons of the unsubstituted trityl phenyl rings appear as an unresolved multiplet between 7.19 and 7.40 ppm. Hydrogen atoms of the phenylene rotator, labeled H16 and H17 in Schemes 1 and 2, appear as a pair of doublets at 7.65 and 7.74 ppm. Signals corresponding to the pentiptycene moiety appear as a singlet at 5.87 ppm for the bridgehead protons (H23) and a doublet of doublets at 6.96 ppm for H26, and the signal for H25 between 7.30 and 7.40 ppm is obscured beneath other aromatic signals between 7.30 and 7.40 ppm. In the asymmetric compound **8**, the bridgehead protons (H23 and H30) give two distinct signals at 5.83 and 5.82 ppm and the proton signals of the hexyl tail (H35−H40) are present between 2.76 and 1.01 ppm. All the ^{13}C NMR spectra matched expectations from their structures. In the case of **1**, all 26 nonequivalent carbons are accounted for. Notably, the chemical shifts of the four alkyne carbons (C14, C13, C19, and C20) appear at 84.7, 86.5, 96.5, and 97.9 ppm, respectively. The phenylene rotator carbons C16 and C17 occur at 131.5 and 131.7 ppm, respectively; however, these carbon signals are not observed in deuterated rotators **1**-d_8 and **3**-d_4 due to signal splitting caused by deuterium substitution. The pentiptycene bridgehead carbons give signals at 52.2, the quaternary trityl carbons at 56.2 ppm, and the methoxy methyl at 55.1 ppm.

Crystal Structure. X-ray diffraction quality single crystals of molecular dirotor **1** were obtained by slow evaporation of a saturated 1:4 toluene/dichloromethane (DCM) solution and were used for X-ray diffraction data acquisition. Diffraction data were obtained with a crystal of **1**-d_8, after the sample of origin had been shown to have identical PXRD patterns to crystals of natural abundance **1**. Evaporation of DCM/diethyl ether, DCM/benzene, and DCM/hexane also yielded crystals but were not of sufficient quality for single crystal X-ray diffraction. Although the crystals obtained from toluene/DCM were shown to include the aromatic solvent (see below), evaporation from

dx.doi.org/10.1021/jo4004053 | J. Org. Chem. 2013, 78, 5293−5302

pure benzene or toluene yielded no crystals. X-ray diffraction data acquired at 100 K from the colorless plates obtained from toluene/DCM were solved in the space group $P\bar{1}$ with only one molecular dirotor and four molecules of toluene per unit cell.[16] As required by the crystal space group, molecules of **1** have a center of symmetry coincident with the one in the triclinic unit cell. As a consequence of this, the two trityl stators have opposing axial chiralities (*M* and *P*), and the two phenylene rotators are equivalent (Figure 2). The alkynes in the structure

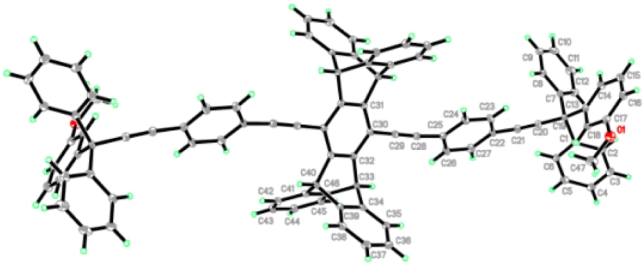

Figure 2. Molecular structure of compound **1** at 100 K with thermal ellipsoids at 50% probability.

deviate significantly from linearity giving **1** an overall S-shape. The torsion angle between rotator phenylenes and the central pentiptycene phenyl ring is 34.2°.

As observed previously for crystals of molecular gyroscopes, which tend to incorporate solvents in the lattice,[17,18] crystals of **1** include four molecules of toluene per unit cell (Figure 3).

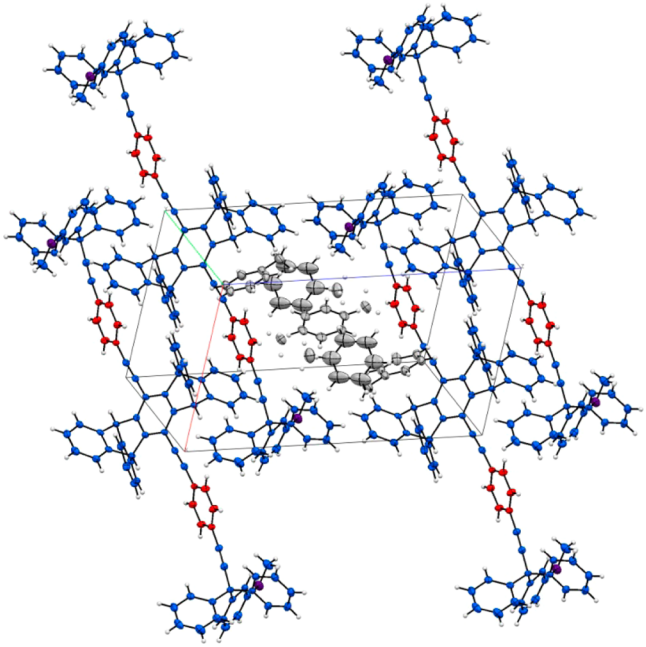

Figure 3. Packing diagram of molecular dirotor **1** illustrating the unit cell. Molecules of **1** are packed in a parallel manner and in layers, with toluene molecules between the layers.

The packing coefficient, given by the van der Waals volume of all the molecules in the unit cell in relation to the total volume of unit cell, is 0.71. The unit cell shows that each phenylene rotator is nested in the cleft of the central pentiptycene stator of a neighboring molecule. It is noteworthy that **1** is packed in a lamellar fashion, with layers of molecular dirotors separated by channels of toluene molecules, which display a high degree of mobility or disorder as evidenced by their larger thermal ellipsoids. Notably, the toluene channels are adjacent to the phenylene rotators and may provide a locally "fluid" region in the crystal which may allow for greater phenylene rotational freedom.

The experimental X-ray powder patterns of **1** and **1**-d_8 are identical to each other but do not have a perfect match to the pattern simulated from the single crystal data (Figure S20, Supporting Information). This may be attributed to the disordered nature and variable content of the toluene clathrate, which tends to escape faster in powder samples. The thermal stability of the crystals was investigated by differential scanning calorimetry (DSC) and thermogravimetric analysis (TGA). The DSC shows an endotherm at 458 °C, which is immediately followed by decomposition (Figure S22, Supporting Information). The TGA curve shows the gradual loss of 8% of the total mass between 70 °C and 180 °C, followed by a more rapid loss of an additional 15% of the total mass between 400 °C and 455 °C (Figure S21, Supporting Information). Both are attributed to the escape of toluene from the crystal lattice.

Solid-State Rotational Dynamics of the Phenylene Group. To realize the electro-optical response depicted in Figure 1, it will be essential to design molecular and crystal architectures where the phenyl groups are able to rotate and reorient. To determine whether or not fast phenylene reorientation is possible within crystals of **1**, we decided to use quadrupolar echo ^{2}H NMR spectroscopy with samples that had the two phenylene groups ^{2}H-labeled. It is well-known that static ^{2}H NMR is one of the most sensitive probes for dynamics in the solid state. The ^{2}H NMR spectrum is dominated by the interaction between the nuclear spin and the electric quadrupole moment at the nucleus.[12,13] The orientation dependence of the quadrupolar coupling characterizes the spectra; each deuteron provides a doublet with a splitting frequency $\Delta\nu$ that depends on the orientation angle β that the C−^{2}H bonds make with respect to the external field:

$$\Delta\nu = {}^3/_4\,(e^2q_{zz}Q/h)(3\cos^2\beta - 1)$$
$$= {}^3/_4\,\mathrm{QCC}(3\cos^2\beta - 1)$$

where Q represents the electric quadrupole moment of the deuteron, e and h are the electric charge and Plank's constant, respectively, and q_{zz} is the magnitude of the principal component of electric field gradient tensor, which lies along the C−^{2}H bond. The combination of these quantities is commonly called the quadrupolar coupling constant (QCC). For aromatic C−^{2}H bonds, QCC = 180 kHz. The peak separation for static deuterons varies from ca. $\Delta\nu$ = 270 kHz when β = 0°, to $\Delta\nu$ = 0 when the C−^{2}H bond is at the magic angle β = 54.7°. In powdered samples, all values of β are represented, but they are not all equally populated; this gives rise to a collection of doublets in all possible orientations, which collectively give a broad symmetric spectrum with two maxima and two shoulders known as a Pake pattern. When the C−^{2}H bonds experience reorientations that reduce the range of their magnetic interactions by dynamic averaging, the shape of the Pake pattern is altered in characteristic ways. It is possible to determine the frequency of the reorientation from ca. 10^4 to 10^8 Hz through line-shape comparison analysis between experimental and simulated spectra. Phenylene rotations in solids are typically modeled in terms of a Brownian exchange between degenerate sites related by 180° rotation, also known

dx.doi.org/10.1021/jo4004053 | J. Org. Chem. 2013, 78, 5293−5302

as 2-fold flips. Spectral changes that occur as a result of this 2-fold phenylene flipping have been well studied in the literature,[19−21] and excellent programs for line-shape simulation are now readily available.[22,23]

Measurements were carried out using a quadrupolar echo pulse sequence on static crystalline powder samples of **1**-d_8. Spectra were obtained at 46.07 MHz with a 90° pulse width of 2.5 μs, echo and refocusing delays of 50 and 42 μs, respectively, a 5 s delay between pulses, and line broadening of 5000 Hz at temperatures ranging from 170 K to 350 K. Some of the data and the best simulations are illustrated in Figure 4. Notably, the

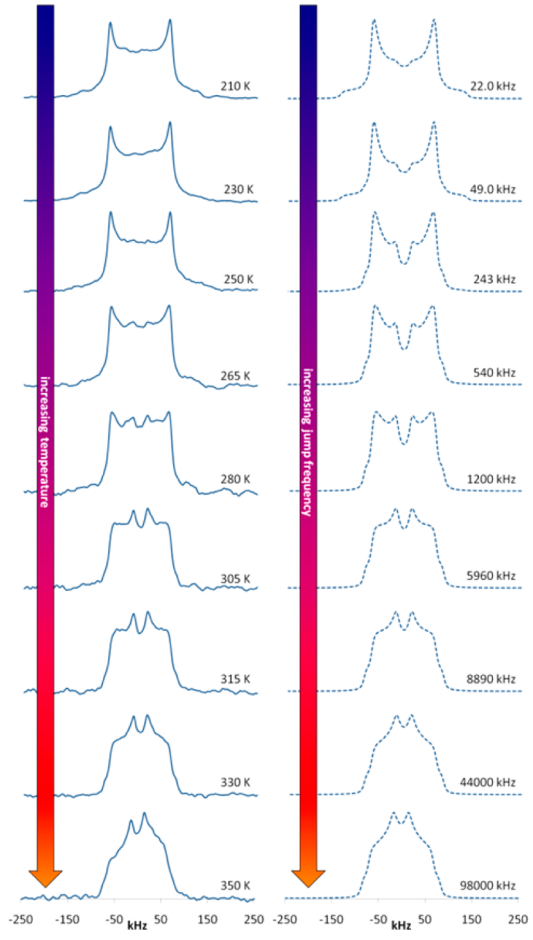

Figure 4. Experimental (left) and simulated (right) solid-state ^{2}H NMR spectra of **1**-d_8. Arrhenius analysis of the rate and temperature data resulted in an average activation energy of 9.0 kcal/mol with a pre-exponential factor of 2.4×10^{13} s^{-1} (Figure S19).

experimental spectra were fitted poorly by simulations that assume a single phenylene jump frequency. A good fit required the use of a log-Gaussian distribution model with a width σ = 1.5, indicating that there is a distribution of activation energies in the sample.[24] It is likely that different environments form as a result of solvent disorder and/or partial desolvation. An Arrhenius plot of the data using the average 2-fold jumping rate constant (Figure S19, Supporting Information) revealed an activation energy of 9.0 kcal/mol with a pre-exponential factor is 2.4×10^{13} s^{-1}. The line-shape differences between the spectra obtained below 210 K were negligible, indicating that motion at these temperatures reaches the slow exchange regime.

Photophysics. It is well-known that the fluorescence of phenyleneethynylenes depends both on the degree of coplanarity between the aromatic rings and the extent of fluorophore aggregation.[8,9,25−27] Theoretical and experimental studies have been performed on these systems to determine the magnitude and the nature of the contribution of planarization. It has been found that when freedom of rotation is allowed and aggregation minimized (i.e., a dilute solution in a nonviscous solvent), the excitation band is heterogeneously broadened while the emission spectrum is vibrationally resolved and relatively narrow. The broadness of the absorption spectrum is determined by a large distribution of phenylene rotamers and the well-resolved emission by a rapid conformational equilibration in the excited state, which gives rise to the dominant contribution from the lowest energy, fully planar rotamer.[8,25] When the rotation of the aryleneethynylenes is restricted and the coplanar rotamer is dominant, as it occurs in stretched poly(ethylene) films, the excitation and absorption spectra become narrow and red-shifted.[8,9] By contrast, when aggregation is present, the red shift is more pronounced and an additional low energy band is sometimes observed.[9,26,28] A single molecule study of a related poly(9,10-anthracenediyle-thynylene-1,4-phenyleneethynylene) has further highlighted the importance of conformation in phenyleneethynylene systems.[29] In addition, density functional theory calculations of 2,5-dimethoxy-*p*-phenyleneethynylene oligomers support the conclusion that twisting about the triple bond leads to a shortening of conjugation length and a widening of the HOMO−LUMO gap.[30] A number of studies have been performed on phenyleneethynylenes with pentiptycene units. These studies have indicated that the incorporation of pentiptycene units into the phenyleneethynylene backbone generally decreases fluorophore aggregation and prevents the corresponding broadening of the emission.[15,28]

To correlate qualitatively the phenylene twist geometries with absorption and emission data, we performed TD-DFT calculations at the B3LYP 6-31G(d) level of theory. The results obtained using a simplified model system consisting of the unadorned BEPEB chromophore are shown in Figure 5a and plotted in Figure 5b. The model considers a frame of reference given by the plane of the central phenylene and explores variations in energy as a function of rotation of one or both aromatic end groups. As shown in Figure 5b, changes in energy for rotation about the alkyne bonds in the ground state are less than 1.0 kcal/mol between the fully coplanar chromophore (Figure 5b, 0° torsion) and that with the two outer phenylenes at a 90° (or −90°) torsion angle. The corresponding energy difference in the excited state is significantly larger, i.e., 9.9 kcal/mol. However, the energy difference is much smaller, 2.7 kcal/mol, when only one of the two outer phenylene rings is rotated by 90° while the other two remain coplanar. The vertical excitation energies calculated in this manner are in good qualitative agreement with experimental data for analogous compounds.[31] We set out to qualitatively validate this trend by comparing the spectra of the BEPEB chromophore containing dirotor **1** with those of model compounds containing BEPE and DEB chromophores in their structures: compounds **8** and **4**, respectively.

The photophysical properties of the three fluorophores **1**, **4**, and **8** are summarized in Table 1, and their fluorescence excitation and emission spectra are shown in Figure 6. Included in the table are the position of the λ_{0-0} bands for absorbance and fluorescent emission, the molar extinction coefficient (ε_{0-0}), and the extinction coefficient at λ = 303 (ε_{303}, the wavelength used to measure fluorescence lifetimes), the

dx.doi.org/10.1021/jo4004053 | J. Org. Chem. 2013, 78, 5293−5302

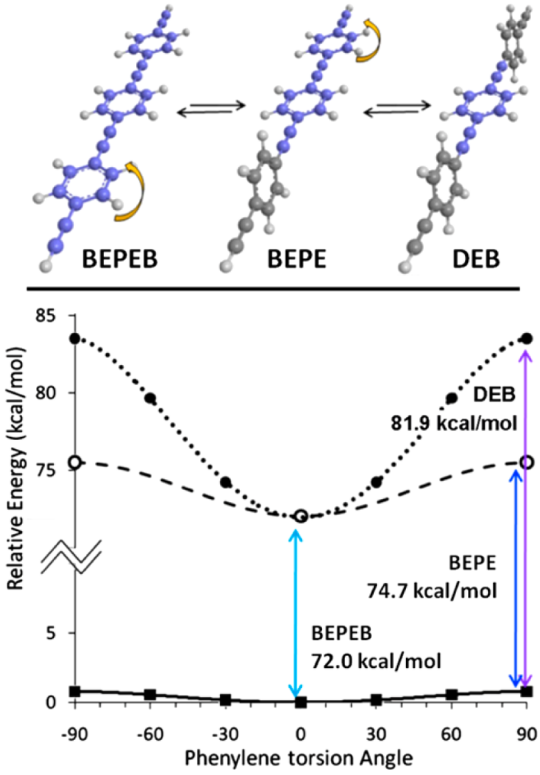

Figure 5. (a) Simplified structure used to calculate the ground and vertical excited-state energies as a function of one and two phenylene torsion angles. (b) Calculated ground-state and excited-state energy surfaces at the TD-DFT B3LYP 6-31G(d) level of theory plotted against one (dashed line) or two (dotted line) phenylene torsion angles. Blue, purple, and violet arrows correspond to the excitation energies of the corresponding BEPEB-, BEPE-, and DEB-like chromophores proposed in Figure 1.

Table 1. Photophysical Properties of the BEPEB, BEPE, and DEB Chromophores in Dirotor 1 and Model Compounds 8 and 4 in Dilute Methylcyclohexane Solutions at Room Temperature

compound	$\lambda_{0-0\ fl}$ (nm)	$\lambda_{0-0\ abs}$ (nm)	$\varepsilon_{0-0\ abs}$ (M^{-1} cm^{-1})	ε_{303} (M^{-1} cm^{-1})	Φ_{fl}	τ_{fl} (ns)
BEPEB **1**	376	369	39437	25866	0.85	≤0.6[a]
BEPE **8**	351	346	20099	18329	0.29	1.4
DEB **4**	342	333	7033	2178	0.70	5.5

[a]Fluorescence lifetimes were shorter than the time resolution of our current instrument.

quantum yield of fluorescence (Φ_{fl}), and the fluorescence lifetime (τ_{fl}). As expected, both the excitation and emission spectra are red-shifted as the number of conjugated aromatic groups and alkyne linkages increases. A red-shift in fluorescence emission of 9 nm was determined from DEB **4** to BEPE **8**, and a shift of 25 nm when comparing BEPE **8** to the full BEPEB chromophore of **1**. This result is in qualitative agreement with the quantum mechanical calculations. The excited-state lifetimes of the three chromophores decrease with increasing conjugation length, while the molar extinction coefficient at $\lambda_{0-0\ abs}$ increases linearly with conjugation length. The fluorescence quantum yields appear to be independent of conjugation length, with BEPE **8** having the lowest quantum

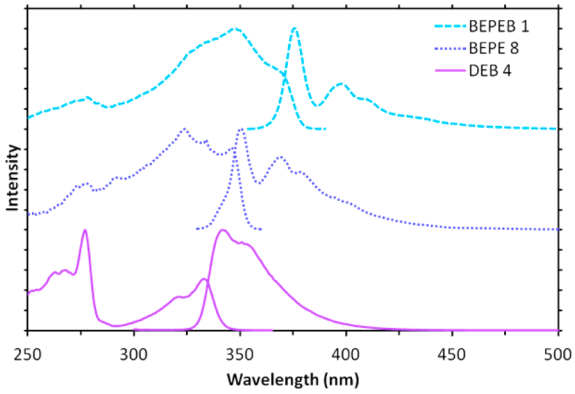

Figure 6. Fluorescence excitation and emission of dirotor BEPEB **1** and model chromophores BEPE **8** and DEB **4** in deoxygenated methylcyclohexane solutions at room temperature.

yield while both BEPEB **1** and DEB **4** have significantly higher yields.

To experimentally determine whether changes in fluorophore planarization result in substantial changes in the emission spectra, one needs conditions where the distribution of twist angles and phenylene rotation is restricted. Considering the relatively flat ground-state rotational energy surface of **1**, one should expect a statistical distribution of all possible phenylene torsion angles to exist in solution, from perfectly planar to perfectly orthogonal. Thus, by flash freezing these solutions it should be possible to capture a "snapshot" of the torsion angle population. To document this, a dilute solution (1.49 μM) of molecular dirotor **1** was prepared in toluene, and its fluorescence spectra were measured both at 298 K and at 77 K (Figure 7). The fluorescence emission spectrum of trimer **1**

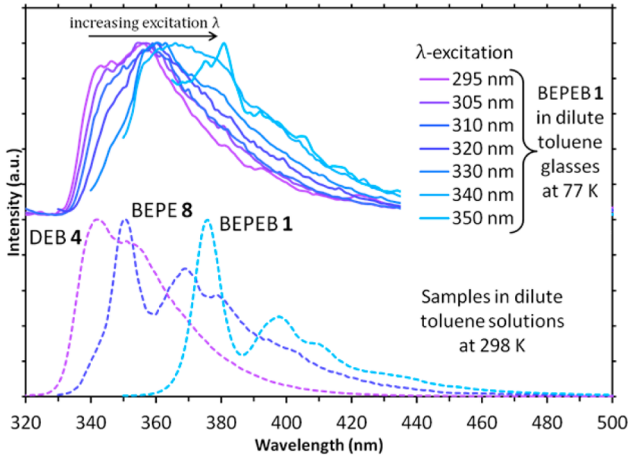

Figure 7. (Top) Fluorescence emission of BEPEB molecular dirotor **1** in frozen toluene at 77K excited at wavelengths that range from 295 to 350 nm, compared to (bottom) the emission spectra of model DEB **4** (violet), model BEPE **8** (purple), and BEPEB dirotor **1** (blue) in toluene at room temperature.

measured at 298 K does not vary as a function of excitation energies and consists of a strong 0−0 band followed by four vibrationally resolved maxima with decreasing intensities. This observation is consistent with a distribution of phenylene angles in the ground state, which are able to equilibrate to the lowest energy coplanar conformation during their excited-state lifetime. Thus, mainly the emission of the lower energy

dx.doi.org/10.1021/jo4004053 | J. Org. Chem. 2013, 78, 5293−5302

coplanar fluorophore is observed, as illustrated by the spectrum shown in cyan color in the bottom part of Figure 7. The spectra corresponding to BEPE **8** and the DEB **4** are increasingly blue-shifted, as shown by the spectra labeled in violet and purple. The fluorescence emission spectrum of BEPEB **1** measured in toluene glasses at 77 K showed the postulated heterogeneity. As phenylene rotation is prevented by the frozen matrix, it is possible to detect a broad range of rotamers by varying the excitation energy. As illustrated in the top frame of Figure 7, excitation at higher energy wavelengths (i.e., 295 nm) preferentially addresses fluorophores that give higher energy emission assigned to the doubly twisted structures that approach the spectral properties of the model DEB **4**. As also shown in the top of Figure 7, a systematic shift in the excitation wavelength from 295 to 350 nm results in a similar shift in the onset of emission. While the spectra are highly heterogeneous and it would be difficult to excite any given species selectively, as the spectrum evolves, it acquires a qualitative resemblance to the spectrum of model BEPE **8** and eventually to that of BEPEB dirotor **1**.

While the fluorescence results from dirotor **1** in solution and in glassy matrix support a strong effect of aromatic torsion angles in the absorption and emission spectra, it was also important to confirm that the BEPEB dirotor **1** remains emissive in the crystalline state. With that in mind, we carried out fluorescence excitation and emission experiments by front-face excitation and detection at 77 K and at 298 K with finely powdered samples of **1** grown from toluene. As illustrated in Figure 8, the solid-state excitation and emission spectra

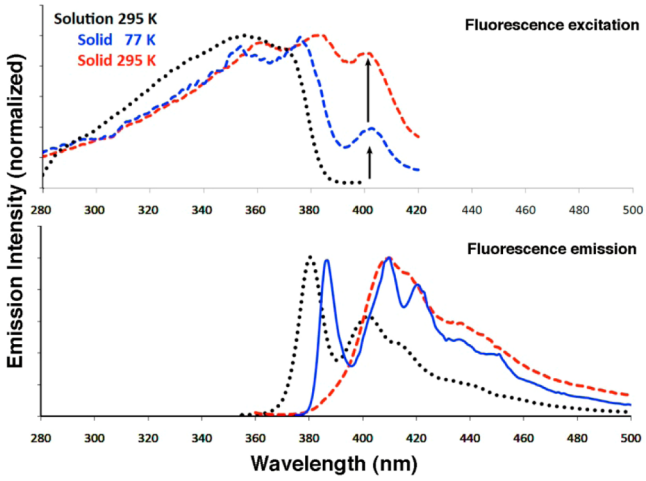

Figure 8. Fluorescence excitation (top) and emission (bottom) spectra of phenyleneethynylene molecular dirotor **1** in solution (black), in the crystalline state at 77 K (blue), and in crystalline state at 298 K (red). The arrow shown in the excitation spectra indicates the thermal population of a red-shifted emissive species in the solid state, which we assign to the fully coplanar conformation.

measured at 77 K (blue spectra) were red-shifted by ca. 10 nm when compared to those measured in solution (black spectra). The solid-state excitation spectrum shows a strong 0−0 transition by ca. 385 nm and an interesting new band at ca. 405 nm. The emission spectrum obtained upon excitation at 405 nm is red-shifted versus that obtained with a 385 nm excitation wavelength (Figure S23, Supporting Information). Notably, an increase in temperature to 298 K resulted in a substantial increase of the 405 nm band and a remarkable change in the shape of the emission envelop where the band of the 0−0 transition by ca. 385 nm disappears. Changes in going from low to high temperature indicate that the high temperature emission (red spectrum) is distorted by self-absorption effects, and, considering the increase in population of the species that absorbs at ca. 405 nm, it is likely that emission occurs from this lower energy species after efficient energy transfer.[32]

To account for the solid-state fluorescence observations, we propose a model based on two distinct absorbing species with equilibrium concentrations that change as a function of temperature. It is reasonable to assume that the major component is the one documented by single crystal X-ray diffraction, with the external phenylene rotators adopting angles of 34.2° with respect to the plane of the phenyl ring in the central pentiptycene. The second and minor component shows the characteristics of a chromophore that is more coplanar and has a lower fluorescence excitation energy. The relative intensities of the band at 420 nm suggest that the population of the minor component increases as a function of temperature, as expected by an increase in mobility within the crystal lattice. In addition, changes in the emission spectrum as function of temperature require that energy transfer from the twisted component to the coplanar species is significantly more favorable at higher temperature. Alternatively, these observations can also be understood as arising from a temperature-dependent reabsorption of the higher energy emission by neighboring chromophores, which could be associated with transient conformational effects related to the high frequency ring oscillations and rotation.

■ CONCLUSIONS

We have presented the synthesis, crystal structure, solid-state dynamics, and photophysical properties of a phenyleneethynylene molecular dirotor **1** and its deuterated isotopologue, **1**-d_8, embedded in the structure of a pentiptycene stator. The role of the bulky pentiptycene is to provide both a central shielding stator and a fixed phenylene, so that the two flanking but linearly conjugated phenylene rotators can explore a variety of torsion angles to affect their excitation energies and photophysical properties in the solid state. X-ray diffraction studies have shown that molecular dirotor **1** is packed in such a manner that all the phenyleneethynylene chromophores are arranged in parallel, so that they all share the same internal rotational axis, as required for the development of functional materials. Variable temperature quadrupolar echo ^{2}H NMR studies have shown that phenylene rotator 2-fold flipping is facile at room temperature, with an activation energy of 9.0 kcal/mol and a Brownian rotational frequency of approximately 2.6 MHz. This energy barrier is lower than those previously shown to help align phenylene flipping with external AC fields, indicating that externally influencing phenylene rotation with an electric field should be feasible in this system.[4c] We have also shown that the phenyleneethynylene chromophore displays a remarkable spectral heterogeneity in rigid glasses, as expected for a chromophore that is capable of displaying significant fluorescence changes as a function of its interphenylene torsion angles. These results provide a very promising platform for the development of molecular dirotors whose amphidynamic nature allows for the rapid shifting of solid-state fluorescence emission and optical properties with the application of an electric field.

dx.doi.org/10.1021/jo4004053 | J. Org. Chem. 2013, 78, 5293−5302

EXPERIMENTAL SECTION

Commercial reagents were used without additional purification. ^{2}H NMR spectra were simulated using the program Express 1.0.[22] A 180° jump model with a quadrupole coupling constant of 180 kHz and an asymmetry parameter of 0.02 was used. A log-Gaussian distribution of 19 phenylene jump rates (σ = 1.5) centered around each nominal phenylene jump rate was generated. A weighted average of the simulated spectra were superimposed to generate the final simulated spectra.

(3-(4-Iodophenyl)-1-(3-methoxyphenyl)prop-2-yne-1,1-diyl)dibenzene 3. A three-neck flask containing 150 mL of THF and 75 mL of diisoproplyamine was purged with argon for 1 h. **2** (1.3 g, 4.4 mmol), 1,4-diiodobenzene (7.18 g, 21.8 mmol), bis-(triphenylphosphine)palladium dichloride (185 mg, 0.264 mmol), and copper iodide (50 mg, 0.528 mmol) were added to the flask, and the reaction mixture was brought to reflux. The reaction mixture was refluxed 12 h, cooled to room temperature, and quenched with saturated aqueous ammonium chloride. The aqueous layer was extracted 2× with DCM. The organic fractions were combined, dried over magnesium sulfate, and evaporated under vacuum. The product was purified by flash chromatography, first using hexanes to elute excess diiodobenzene and switching to 2:1 hexanes:DCM to elute 1.34 g (61%) of the colorless solid product: mp 120.6−121.4 °C; ^{1}H NMR (300 MHz, $CDCl_3$) δ 7.60 (d, J = 8.1, 2H), 7.27−7.15 (m, 13H), 6.86−6.81 (m, 2H), 6.76 (d, J = 8.1, 2.4, 1H), 3.69 (s, 3H); ^{13}C NMR (75 MHz, $CDCl_3$) δ 159.3, 146.6, 144.9, 137.4, 133.1, 129.1, 128.9, 128.0, 126.9, 123.0, 121.7, 115.5, 111.9, 97.0, 93.7, 84.2, 56.1, 55.1; IR (DRIFT cm^{-1}) 3058, 3026, 2997, 2965, 2937, 2834, 1604, 1579, 1482, 1445, 1433, 1289, 1241, 1049, 816, 747, 695; MS (ESI/APCI m/z) calculated for $C_{28}H_{21}IO$+H 501.0715, found 501.0710.

(3-(d_4-4-Bromophenyl)-1-(3-methoxyphenyl)prop-2-yne-1,1-diyl)dibenzene 3-d_4. A three-neck flask containing 100 mL of tetrahydrofuran and 50 mL of diisopropylamine was purged with argon for 2 h. **2** (995 mg, 3.3 mmol), d_4-1,4-dibromobenzene (3225 mg, 13.5 mmol), bis(triphenylphosphine)palladium dichloride (121 mg, 0.17 mmol), and copper iodide (157 mg, 0.82 mmol) were added to the flask, and the flask was purged for another 10 min. The reaction mixture was heated to reflux for 18 h, and it was then cooled and quenched with saturated ammonium chloride. The crude product was extracted into dichloromethane and dried over anhydrous magnesium sulfate. The solvent was evaporated under reduced pressure, and the residue was redissolved in dichloromethane and loaded onto a silica gel column. The product was eluted with hexanes/dichloromethane, with a gradient from 80:20 to 50:50. The solvent was evaporated, to give a colorless solid (1.01 g, 60%). Excess d_4-1,4-dibromobenzene (2.11 g) was recovered with high purity: mp 118.3−119.6 °C; ^{1}H NMR ($CDCl_3$, 300 MHz) δ 7.32−7.24 (m, 10H), 7.22 (t, J = 8.0 Hz, 1H), 6.90 (m, 2H), 6.81 (ddd, J = 8.1, 2.4, 0.9 Hz, 1H), 3.73 (s, 3H); ^{13}C ($CDCl_3$, 75 MHz) δ 159.4, 146.7, 145.0, 129.1, 129.0, 128.1, 127.0, 122.3, 122.0, 121.8, 115.6, 111.9, 96.8, 84.0, 56.2, 55.2; IR (DRIFT cm^{-1}) 3085, 3065, 3045, 3026, 3015, 2955, 2932, 2903, 2835, 1598, 1578, 1482, 1446, 1432, 1287, 1255, 1050, 756, 736, 697; mass (MALDI m/z) calculated for $C_{28}H_{17}D_4BrO$ 456.10, found 456.32.

6,13-Bis((4-(3-(3-methoxyphenyl)-3,3-diphenylprop-1-yn-1-yl)phenyl)ethynyl)-5,7,12,14-tetrahydro-5,14:7,12-bis([1,2]-benzeno)pentacene 1. Diethynylpentiptycene **4** (159 mg, 0.33 mmol) was dispersed in 75 mL of tetrahydrofuran and purged with argon in an addition funnel for 1 h. **3** (500 mg, 1.0 mmol), bis(triphenylphosphine)palladium dichloride (23.4 mg, 0.033 mmol), and copper iodide (3.2 mg, 0.017 mmol) were dissolved in 75 mL of tetrahydrofuran and 75 mL of diisopropylamine in a three-neck flask, purged with argon for 1 h and heated to reflux. Diethynylpentiptycene **4** dispersion was added over 6 h, and a 10 mL portion of THF was used to rinse residual pentiptycene into the reaction flask. The reaction was allowed to continue at reflux for another 1 h at which point **4** had been consumed by TLC. The reaction was then quenched with saturated ammonium chloride and extracted into dichloromethane, dried over anhydrous magnesium sulfate, and evaporated under reduced pressure. The residue was purified by column chromatography with a 70:30 to 60:40 hexanes:DCM eluent. The solvent was evaporated under reduced pressure to yield **1** as a white powder with strong violet fluorescence (134 mg, 33%). Crystallization of **1** by slow evaporation of a 4:1 DCM:toluene mixture afforded small square crystals: mp (decomp); ^{1}H NMR ($CDCl_3$, 500 MHz) δ 7.74 (d, J = 8.1, 4H), 7.65 (d, J = 8.1, 4H), 7.4−7.26 (m, 30H), 6.98−6.93 (m, 12H), 6.87−6.85 (dd, J = 8.1, 1.7 Hz, 2H), 5.87 (s, 4H), 3.79 (s, 6H); ^{13}C NMR ($CDCl_3$, 125 MHz) δ 159.3, 146.6, 144.9, 144.7, 144.0, 131.7, 131.5, 129.1, 128.9, 128.0, 126.9, 125.2, 123.9, 123.7, 122.8, 121.7, 115.5, 114.6, 111.9, 97.9, 96.5, 86.5, 84.7, 56.2, 55.1, 52.2; IR (DRIFT cm^{-1}) 3062, 3020, 2968, 2930, 1598, 1488, 1458, 1290, 1248, 1181, 1035, 836, 751, 697; MS (ESI/APCI m/z) calculated for $C_{94}H_{62}O_2$+NH_4 1240.5093, found 1240.5088.

1-d_8: Diethynylpentiptycene **4** (207 mg, 0.43 mmol) was dispersed in 75 mL of tetrahydrofuran and purged with argon in an addition funnel for 1 h. **3**-d_4 (596 mg, 1.3 mmol), bis(triphenylphosphine) palladium dichloride (30.2 mg, 0.043 mmol), and copper iodide (4.1 mg, 0.0215 mmol) were dissolved in 75 mL of tetrahydrofuran and 75 mL of diisopropylamine in a three-neck flask, purged with argon for 1 h, and heated to reflux. Diethynylpentiptycene **4** dispersion was added over 24 h, and a 10 mL portion of THF was used to rinse residual pentiptycene into the reaction flask. The reaction was allowed to continue at reflux for another 24 h, and it was then quenched with saturated ammonium chloride, extracted into dichloromethane, dried over anhydrous magnesium sulfate, and evaporated under reduced pressure. The residue was purified by column chromatography with a 60:40 hexanes:DCM eluent. The solvent was evaporated under reduced pressure to yield **1**-d_8 as a white powder with strong violet fluorescence (288 mg, 54%). Crystallization of **1**-d_8 by slow evaporation of a 4:1 DCM:toluene mixture afforded small square crystals. Anal.: mp decomposes; ^{1}H NMR ($CDCl_3$, 500 MHz) δ 7.39−7.33 (m, 24H), 7.32−7.30 (m, 4H), 7.28 (t, J = 8.0 Hz, 2H), 6.99−6.93 (m, 12H), 6.87 (dd, J = 8.5, 2.5, 2H), 5.87 (s, 4H), 3.79 (s, 6H); ^{13}C ($CDCl_3$, 125 MHz) δ 159.7, 146.9, 145.2, 144.9, 144.2, 129.4, 129.2, 128.3, 127.2, 125.5, 124.0, 122.9, 122.0 115.8, 115.0, 112.2, 98.2, 96.7, 86.8, 84.9, 56.5, 55.4, 53.6, 52.5; IR (DRIFT cm^{-1}) 2955, 2922, 2853, 1599, 1457, 1251, 1051; MS (MALDI) calculated for $C_{94}H_{54}D_8O_2$ 1230.53, found 1230.53.

6-Ethynyl-13-(oct-1-yn-1-yl)-5,7,12,14-tetrahydro-5,14:7,12-bis([1,2]benzeno)pentacene 7. Pentiptycene quinone **3** (50 mg, 0.11 mmol) is dissolved in dry THF in a flame-dried flask under argon. To generate 1-octynyllithium solution, 1-octyne (103 mg, 0.93 mmol) was dissolved in 8 mL of dry THF in a flame-dried flask under argon, the solution was cooled to −78 °C, and n-butyllithium (0.5 mL, 1.6 M in hexane, 0.80 mmol) was added. 1-Octynyllithium solution was titrated into the pentiptycene quinone **3** solution at −78 °C until TLC showed that pentiptycene quinone **3** was completely consumed. A solution of trimethylsilylethynyllithium was prepared by adding n-butyllithium (0.5 mL, 1.6 M in hexane, 0.80 mmol) to a solution of ethynyltrimethylsilane (88 mg, 0.90 mmol) in 8 mL of dry THF at −78 °C. Trimethylsilylethynyllithim solution was titrated into the monoreacted pentiptycene quinone until it was consumed as shown by TLC. The reaction mixture was warmed to room temperature, acidified with 1 M HCl, extracted into DCM, and washed with water. The organic layer was dried over magnesium sulfate and evaporated to yield the crude asymmetric diol. This product dissolved in acetone and was stirred overnight at room temperature with a solution of tin(II) chloride hydrate (69 mg, 0.27 mmol) in 50% acetic acid to give the rearomatized asymmetrical diyne. The reaction mixture was extracted into DCM, the organic layer was washed with a saturated solution of sodium bicarbonate, and the organic layer was dried over magnesium sulfate and evaporated. The product mixture was purified by preparatory TLC (80:20 hexane/DCM) and found to contain a 1:2 mixture of TMS-protected diyne **6** and deprotected terminal diyne **7**. Both products were redissolved in THF and stirred overnight at room temperature with an excess of potassium hydroxide in water. The reaction mixture was washed with brine, the brine layer was re-extracted with DCM, and the combined organic layers were washed with brine, dried over magnesium sulfate, and then evaporated to give **7** as a waxy yellow solid (29 mg, 48%): mp 109.6−112.3 °C; ^{1}H NMR (500 MHz, $CDCl_3$) δ 7.36−7.32 (m, 8H), 6.94−6.93 (m, 8H), 5.81 (s,

dx.doi.org/10.1021/jo4004053 | J. Org. Chem. 2013, 78, 5293−5302

2H), 5.79 (s, 2H), 3.66 (s, 1H), 2.75 (t, J = 6.7 Hz, 2H), 1.87 (pent, J = 7.2 Hz, 2H), 1.76 (pent, J = 7.2 Hz, 2H), 1.53−1.48 (m, 4H), 1.01 (t, J = 7.0 Hz, 3H); ^{13}C ($CDCl_3$, 125 MHz) δ 144.9, 144.8, 144.2, 143.6, 125.2, 125.1, 123.7, 123.6, 116.1, 112.6, 98.15, 83.9, 79.2, 75.9, 52.0, 51.9, 31.4, 29.0, 28.7, 22.7, 19.8, 14.1; IR (DRIFT cm^{-1}) 3297, 3069, 3043, 3022, 2960, 2927, 2855, 2150, 1680, 1458, 1260, 1088, 1017; mass (ESI/APCI m/z) calculated for $C_{44}H_{34}$+NH_4^+ 580.3004, found 580.3023.

6-((4-(3-(3-Methoxyphenyl)-3,3-diphenylprop-1-yn-1-yl)-phenyl)ethynyl)-13-(oct-1-yn-1-yl)-5,7,12,14-tetrahydro-5,14:7,12-bis([1,2]benzeno)pentacene 8. A solution of 8 mL of diisopropylamine in 16 mL of THF was purged with argon in a three-neck flask. After 1 h, asymmetrical pentiptycene **7** (29 mg, 0.5 mmol), half-rotor **3** (31 mg, 0.06 mmol), bis(triphenylphospnene)palladium dichloride (3.5 mg, 0.005 mmol), and copper iodide (0.6 mg, 0.003 mmol) were added quickly to the purged solvents, and the mixture was purged with argon for an additional 0.5 h. The reaction mixture was stirred at reflux for 12 h under argon. The cooled reaction mixture was washed with saturated ammonium chloride, the ammonium chloride was extracted with DCM, and the combined organic layers were washed with brine, dried over magnesium sulfate, and evaporated under reduced pressure. The product was purified by preparatory TLC by three subsequent elutions with 80:20 hexane/DCM. The product **8** was isolated as an off-white solid (13 mg, 27%): mp (decomp); ^{1}H NMR (500 MHz, $CDCl_3$) δ 7.73 (d, J = 8.1 Hz, 2H), 7.64 (d, J = 8.1 Hz, 2H), 7.40−7.26 (m, 19H), 6.98 (t, J = 2.0 Hz, 1H), 6.96−6.93 (m, 9H), 6.85 (dd, J = 8.0, 2.5 Hz, 1H), 5.83 (s, 2H), 5.82 (s, 2H), 3.79 (s, 3H), 2.76 (t, J = 6.7 Hz, 2H), 1.88 (pent, J = 7.3 Hz, 2H), 1.77 (pent, J = 7.3 Hz, 2H), 1.56−1.50 (m, 4H), 1.01 (t, J = 7.0 Hz, 3H); ^{13}C ($CDCl_3$, 125 MHz) δ 159.4, 146.8, 145.1, 145.0, 144.9, 143.8, 143.7, 131.8, 131.6, 129.2, 129.0, 128.1, 127.0, 125.2 (two carbons with coincident chemical shifts), 123.8, 123.8, 123.7, 123.1, 121.8, 115.9, 115.6, 113.7, 112.0, 98.3, 97.8, 96.0, 86.8, 84.8, 76.2, 56.3, 55.2, 52.3, 52.1, 31.6, 29.7, 28.8, 22.8, 20.0, 14.2; IR (DRIFT cm^{-1}) 3063, 6022, 2960, 2921, 2851, 1723, 1598, 1584, 1458, 1258, 1084, 1023; mass (ESI/APCI m/z) calculated for $C_{72}H_{54}O$+NH_4^+ 952.4518, found 952.4542.

■ ASSOCIATED CONTENT

Ⓢ Supporting Information

Spectroscopic data (^{1}H, ^{13}C NMR, FTIR) for compounds **3**, **3**-d_4, 1,1-d_8, **7**, and **8**. Crystallographic information file (cif) for compound **1**. DSC, TGA, PXRD, and solid-state fluorescence plots. Computational details. This material is available free of charge via the Internet at http://pubs.acs.org.

■ AUTHOR INFORMATION

Corresponding Author

*E-mail: mgg@chem.ucla.edu.

Notes

The authors declare no competing financial interest.

■ ACKNOWLEDGMENTS

This work was supported by NSF IGERT: Materials Creation Training Program (MCTP) − DEG-0654431 and the California NanoSystems Institute and by grants DMR1101934 and CHE0-844455.

■ REFERENCES

(1) (a) Coskun, A.; Banaszak, M.; Astumian, R. D.; Stoddart, J. F.; Grzybowski, B. A. *Chem. Soc. Rev.* **2012**, *41*, 19. (b) Michl, J.; Sykes, E. C. H. *ACS Nano* **2009**, *3*, 1042. (c) Balzani, V.; Credi, A.; Venturi, M. *Molecular Devices and Machines*, 2nd ed.; Wiley: Weinheim, 2008. (d) Kay, E. R.; Leigh, D. A.; Zerbetto, F. *Angew. Chem., Int. Ed.* **2007**, *46*, 72. (e) Browne, W. R.; Feringa, B. L. *Nat. Nanotechnol.* **2006**, *1*, 25. (f) Karlen, S. D.; Garcia-Garibay, M. A. *Top. Curr. Chem.* **2006**, *262*, 179. (g) Astumian, R. D. *Science* **1997**, *276*, 917.

(2) (a) Vogelsberg, C. S.; Garcia-Garibay, M. A. *Chem. Soc. Rev.* **2012**, *41*, 1892. (b) Garcia-Garibay, M. A. *Nat. Mater.* **2008**, *7*, 431. (c) Akutagawa, T.; Nakamura, T. *Dalton Trans.* **2008**, 6335−6345. (d) Garcia-Garibay, M. A. *Angew Chem., Int. Ed.* **2007**, *46*, 8945. (e) Khuong, T.-A. V.; Nuñez, J. E.; Godinez, C. E.; Garcia-Garibay, M. A. *Acc. Chem. Res.* **2006**, *39*, 413. (f) Garcia-Garibay, M. A. *Proc. Natl. Acad. Sci. U.S.A.* **2005**, *102*, 10793.

(3) (a) Irie, B.; Morimoto, M.; Irie, M. *J. Am. Chem. Soc.* **2010**, *132*, 14172. (b) Zhu, L.; Al-Kaysi, R. O.; Bardeen, C. J. *J. Am. Chem. Soc.* **2011**, *133*, 12569. (c) Zhu, L.; Al-Kaysi, R. O.; Dillon, R. J.; Tham, F. S.; Bardeen, C. J. *Cryst. Growth Des.* **2011**, *11*, 4975. (d) Naumov, P.; Kowalik, J.; Solntsev, K. M.; Baldridge, A.; Moon, J.-S.; Kranz, C.; Tolbert, L. M. *J. Am. Chem. Soc.* **2010**, *132*, 5845. (e) Koshima, H.; Ojima, N.; Uchimoto, H. *J. Am. Chem. Soc.* **2009**, *131*, 6890. (f) Kobatake, S.; Takami, S.; Muto, H.; Ishikawa, T.; Irie, M. *Nature* **2007**, *446*, 778. (g) Brown, M. E.; Hollingsworth, M. D. *Nature* **1995**, *376*, 323.

(4) (a) Ye, Q.; Takahashi, K.; Hoshino, N.; Kikuchi, T.; Akutagawa, T.; Noro, S.-I.; Takeda, S.; Nakamura, T. *Chem.—Eur. J.* **2011**, *17*, 14442. (b) Winston, E. B.; Lowell, P. J.; Vacek, J.; Chocholousova, J.; Michl, J.; Price, J. C. *Phys. Chem. Chem. Phys.* **2008**, *10*, 5188. (c) Horansky, R. D.; Clarke, L. I.; Winston, E. B.; Price, J. C.; Karlen, S. D.; Jarowski, P. D.; Santillan, R.; Garcia-Garibay, M. A. *Phys. Rev. B* **2006**, *74*, 054306. (d) Horansky, R. D.; Clarke, L. I.; Price, J. C.; Khuong, T.-A. V.; Jarowski, P. D.; Garcia-Garibay, M. A. *Phys. Rev. B* **2005**, *72*, 014302.

(5) (a) Akutagawa, T.; Shitagami, K.; Nishihara, S.; Takeda, S.; Hasegawa, T.; Nakamura, T.; Hosokoshi, Y.; Inoue, K.; Ikeuchi, S.; Miyazaki, Y.; Saito, K. *J. Am. Chem. Soc.* **2005**, *127*, 4397. (b) Akutagawa, T.; Sato, D.; Koshinaka, H.; Aonuma, M.; Noro, S.-I.; Takeda, S.; Nakamura, T. *Inorg. Chem.* **2008**, *47*, 5951. (c) Ye, Q.; Akutagawa, T.; Noro, S.-I.; Nakamura, T.; Xiong, R.-G. *Cryst. Growth Des.* **2010**, *10*, 4856.

(6) Ko, C.-C.; Yam, V. W.-W. Photoswitching Materials. In *Supramolecular Chemistry: From Molecules to Nanomaterials*; Gale, P. A.; Steed, J. W., Eds.; Wiley: New York, 2012; Vol. *5*; p 2643.

(7) (a) Godinez, C. E.; Zepeda, G.; Garcia-Garibay, M. A. *J. Am. Chem. Soc.* **2002**, *124*, 4701. (b) Karlen, S. D.; Ortiz, R.; Chapman, O. L.; Garcia-Garibay, M. A. *J. Am. Chem. Soc.* **2005**, *127*, 6554. (c) Khuong, T.-A.; Nuñez, J.; Godinez, C.; Garcia-Garibay, M. *Acc. Chem. Res.* **2006**, *39*, 413.

(8) (a) Levitus, M.; Schmieder, K.; Ricks, H.; Schimizu, K. D.; Bunz, U. H. F.; Garcia-Garibay, M. A. *J. Am. Chem. Soc.* **2001**, *123*, 4259. (b) Levitus, M.; Schmieder, K.; Ricks, H.; Schimizu, K. D.; Bunz, U. H. F.; Garcia-Garibay, M. A. *J. Am. Chem. Soc.* **2002**, *124*, 8181. (c) Schmieder, K.; Levitus, M.; Dang, H.; Garcia-Garibay, M. A. *J. Phys. Chem. A* **2002**, *106*, 1551.

(9) (a) Yang, J.-S.; Yan, J.-L.; Lin, C. K.; Chen, C.-Y.; Chiou, S.-Y.; Liau, K. L.; Gavin Tsai, H. H.; Lee, G. H.; Peng, S. M. *J. Am. Chem. Soc.* **2006**, *128*, 14109. (b) Yang, J.-S.; Yan, J.-L.; Lin, C. K.; Chen, C.-Y.; Xie, Z.-X.; Chen, C.-H. *Angew. Chem., Int. Ed.* **2009**, *48*, 9936.

(10) (a) Collings, P. J.; Hird, M. *Introduction to Liquid Crystals*; Taylor and Francis, Ltd.: London, 1997. (b) Blinov, L. M. *Electrooptic and Magneto-Optical Properties of Liquid Crystals*; Wiley: New York, 1983.

(11) (a) Garcia-Garibay, M. A.; Godinez, C. E. *Cryst. Growth Des.* **2009**, *9*, 3124. (b) Lemouchi, C.; Vogelsberg, C. S.; Zorina, L.; Simonov, S.; Batail, P.; Brown, S.; Garcia-Garibay, M. A. *J. Am. Chem. Soc.* **2011**, *133*, 6371.

(12) Hoatson, G. L.; Vold, R. L. *NMR: Basic Princ. Prog.* **1994**, *32*, 1−67.

(13) Fyfe, C. A. *Solid State NMR for Chemists*; CFC Press: Guelph, Ontario, 1983.

(14) Commins, P.; Nuñez, J. E.; Garcia-Garibay, M. A. *J. Org. Chem.* **2011**, *76*, 8355.

(15) Yang, J.; Swager, T. M. *J. Am. Chem. Soc.* **1998**, *120*, 11864.

(16) Crystallographic parameters of **1**: Empirical formula at 100(2) K: $C_{94}H_{62}O_2{\cdot}4(C_7H_8)$, formula weight: 1591.97, space group: $P\bar{1}$, Z = 1, a = 10.562(2) Å, b = 12.190(2) Å, c = 18.671(4) Å, α = 95.819(2)°,

β = 105.130(2)°, γ = 103.746(3)°, V = 2219.6(7) Å^3, R = 7.26%, $w2R$ = 17.22%.
(17) Dominguez, Z.; Dang, H.; Strouse, J. M.; Garcia-Garibay, M. A. *J. Am. Chem. Soc.* **2002**, *124*, 7719.
(18) Godinez, C. E.; Zapeda, G.; Mortko, C. J.; Dang, H.; Garcia-Garibay, M. A. *J. Org. Chem.* **2003**, *69*, 1652.
(19) Cholli, A. L.; Dumais, J. J.; Engel, A. K.; Jelinski, L. W. *Macromolecules* **1984**, *17*, 2399.
(20) Rice, D. M.; Witebort, R. J.; Griffin, R. G.; Meirovich, E.; Stimson, E. R.; Meinwald, Y. C.; Freed, J. H.; Scheraga, H. A. *J. Am. Chem. Soc.* **1981**, *103*, 7707.
(21) Rice, D. M.; Meinwald, Y. C.; Scheraga, H. A.; Griffin, R. G. *J. Am. Chem. Soc.* **1987**, *109*, 1636.
(22) The simulation program NMR-WEBLAB from the Spiess lab is available on the web: Macho, V.; Brombacher, L.; Spiess, H. W. *Appl. Magn. Reson.* **2001**, *20*, 405.
(23) The program Express 1.0 from the Vold lab is also available on the web: Vold, R. L.; Hoatson, G. L. *J. Magn. Reson.* **2009**, *198*, 57.
(24) Comotti, A.; Bracco, S.; Valsesia, P.; Beretta, M.; Sozzani, P. *Angew. Chem., Int. Ed.* **2010**, *49*, 1760.
(25) Sluch, M. I.; Godt, A.; Bunz, U. H. F.; Berg, M. A. *J. Am. Chem. Soc.* **2001**, *123*, 6447.
(26) Kim, J.; Levitsky, I. A.; McQuade, D. T.; Swager, T. M. *J. Am. Chem. Soc.* **2002**, *124*, 7710.
(27) Nakayama, H.; Kimura, S. *J. Phys. Chem. A* **2011**, *115*, 8960.
(28) Kim, J.; Swager, T. M. *Nature* **2001**, *411*, 1030.
(29) Shinohara, K.; Yamaguchib, S.; Wazawa, T. *Polymer* **2001**, *42*, 7915.
(30) Li, N.; Jia, K.; Wang, S.; Xia, A. *J. Phys. Chem. A* **2007**, *111*, 9393.
(31) Khan, M. S.; Kakkar, A. K.; Long, N. J.; Lewis, J.; Raithby, P.; Nguyen, P.; Marder, T. B.; Wittmann, F.; Friend, R. H. *J. Mater. Chem.* **1994**, *4*, 1227.
(32) Lakowicz, J. *Principles of Fluorescence Spectroscopy*, 2nd ed.; Springer: Baltimore, MD, 2004.